

THE 13<sup>TH</sup> INTERNATIONAL STELLARATOR WORKSHOP

Exploring Stellarator Configuration Space with Global Search Methods

Mynick, H.,<sup>1</sup> Pomphrey,<sup>1</sup> N., Ethier, S.<sup>1</sup>

<sup>1</sup>Princeton Plasma Physics Laboratory, Princeton University, Princeton, NJ 08543, USA

E-mail: mynick@pppl.gov

**Abstract:** An exploration of stellarator configuration space  $\mathbf{z}$  for quasi-axisymmetric stellarator (QAS) designs is discussed, using methods which provide a more global view of that space. To this end, we have implemented a "differential evolution" (DE) search algorithm in an existing stellarator optimizer, which is much less prone to become trapped in local, suboptimal minima of the cost function  $\chi$  than the local search methods used previously. This search algorithm is complemented by mapping studies of  $\chi$  over  $\mathbf{z}$  aimed at gaining insight into the results of the automated searches. We find that a wide range of the attractive QAS configurations found previously fall into a small number of classes, with each class corresponding to a basin of  $\chi(\mathbf{z})$ . We develop maps on which these earlier stellarators can be placed, the relations among them seen, and understanding gained into the physics differences between them. It is also found that, while still large, the region of  $\mathbf{z}$  space containing practically realizable QAS configurations is much smaller than earlier supposed.

## Introduction

The search for attractive stellarator designs has been greatly enhanced by the development of optimization codes which search configuration space  $\mathbf{z}$  using a specified cost function  $\chi(\mathbf{z})$ . Such codes have been used extensively in the design of W7-X,[1] HSX,[2] and more recently, for designing the proposed quasi-axisymmetric stellarator (QAS) NCSX.[3] Here, we discuss an exploration of  $\mathbf{z}$  space for QASs using methods which provide a more global view of that space than earlier 'local' search methods, such as the Levenberg-Marquardt (LM) method[4] used in the present NCSX optimizer Stellopt. To this end, we have implemented a "differential evolution" (DE) search algorithm[5] into Stellopt, yielding an optimizer "Stellopt-DE" which is much less prone to become trapped in local, suboptimal minima of  $\chi(\mathbf{z})$  than those using local methods. This search algorithm is complemented by mapping studies of  $\chi$  over  $\mathbf{z}$  aimed at gaining insight into the results of the automated searches. A fuller discussion of the studies described here is given in [6].

The DE algorithm is similar to genetic algorithms,[7] but suited to exploration of a continuous space. Unlike local methods, these do not require taking derivatives, but evolve a sequence of generations  $g=0, \dots, g_{\max}$ , each generation comprised of an ensemble of  $N_p$  system points  $\mathbf{z}^i(g)$  distributed over  $\mathbf{z}$  space, and with a simple rule for obtaining the  $(g+1)^{\text{th}}$  generation from the  $g^{\text{th}}$ . Because the evolution is of a cloud of system points, rather than of a single point along one trajectory, the evolution of the DE population can provide a less myopic map of the  $\mathbf{z}$  space topography compared with that from traditional local algorithms.

Obtaining such a map of  $\mathbf{z}$  space is important, both for understanding, and for finding optimal designs. Up to now, the LM optimizer (Stellopt-LM) has obtained promising QAS configurations after a complicated sequence of optimizer runs and human adjustments, and there has been little knowledge of how many different types of good QAS designs there may be and what their distinguishing features are. By mapping  $\chi$  over  $\mathbf{z}$  space, we find that a wide range of the attractive QAS configurations previously studied falls into a small number of classes, with each class corresponding to a 'basin' of  $\chi$ . The maps also indicate that, while the full  $\mathbf{z}$  space is

in principal enormous, the region of that space containing configurations which are practically realizable is much smaller than one might have supposed (though still large).

### Stellopt-DE Applications

The cost function  $\chi(\mathbf{z})$  is given in Stellopt by  $\chi^2 = \sum_i \chi_i^2 = \sum_i w_i^2 \hat{\chi}_i^2$ , where the  $w_i$  are the weights of the various contributions  $\hat{\chi}_i^2$  to  $\chi^2$ . Equilibria are computed with VMEC, and then additional codes are called to compute the different  $\hat{\chi}_i^2$ , including Terpsichore for the kink component  $\chi_k^2$ , and COBRA for the ballooning component  $\chi_B^2$ . Confinement quality is gauged by the quasisymmetry measure  $\chi_{Bmn}^2 \equiv \langle \sum_{m,n \neq 0} B_{mn}^2 / B_{00}^2 \rangle_s$ , where the  $B_{mn}$  are the Fourier amplitudes of magnetic field strength  $B$ .

To illustrate the features of a DE search, we show a DE study paralleling a series of LM studies done [8] to investigate the operational flexibility of the reference NCSX configuration LI383, using the "M1017" set of modular coils. This calculation thus uses VMEC in free-boundary mode, and  $\mathbf{z}$  space has dimension  $D=11$ . For  $j=1-9$ ,  $z_j=I_j$  are the currents in the 4 distinct types of modular coils, in the 1 set of auxiliary TF coils, and 4 equivalent currents for the multipole fields used to represent the PF contribution to  $\mathbf{B}$ . Following the heuristic rules as in [5] we take the number  $N_p$  of members in a generation  $\approx 7 \times D = 80$ .

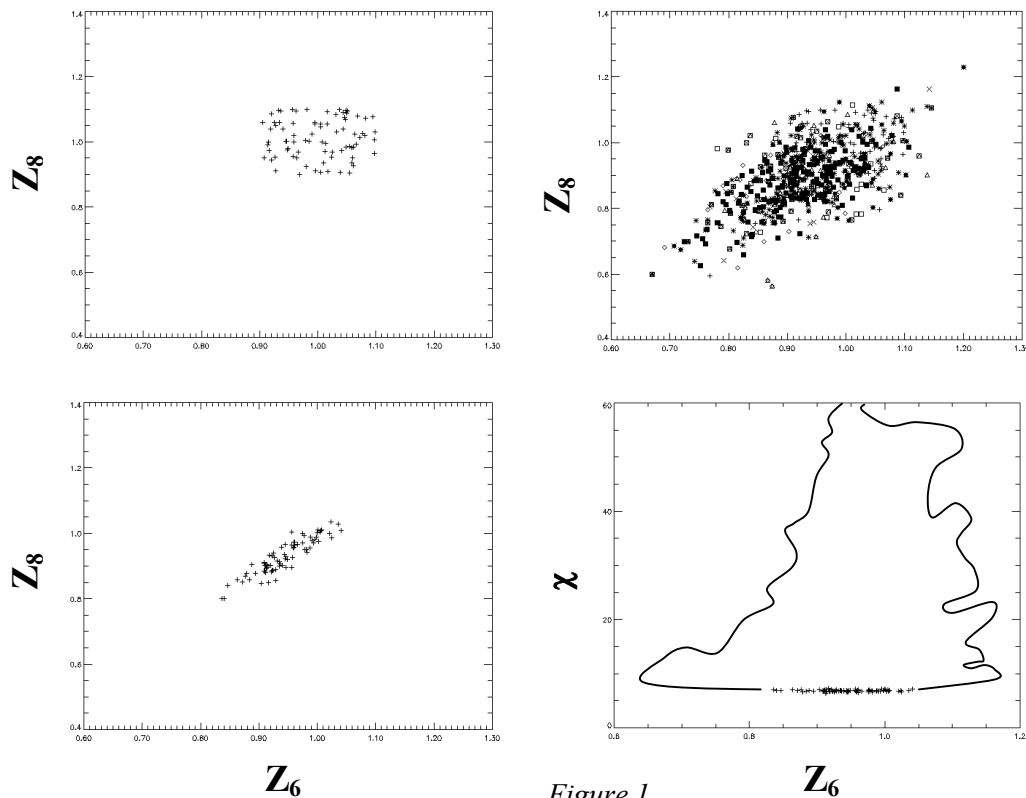


Figure 1

In Fig.1(a-c) are shown projections of the DE population onto 2 particular  $z_j$ ,  $j=6$  and 8, (a) for generation  $g=0$ , (b) for the superposition of generations  $g=0-49$ , and (c) for  $g=49$ . The choice of  $z_j$  used for plotting is arbitrary, and the appearance is similar for

other pairs. The initialization randomly selects  $z_j$  values between 0.8 and 1.2 times those for LI383, producing the rectangular filled region in Fig.1a. Between  $g=0$  and  $g=49$ , the ensemble spreads as the algorithm searches  $\mathbf{z}$  space, as seen in Fig.1b. This is followed by a dimensional contraction to the nearly 1-D form shown in Fig.1c. Finally, in Fig.1d is shown the cost function value  $\chi(\mathbf{z})$  versus  $z_6$  for  $g=49$ , with the boundary line showing the locus of the cloud of values which would appear for the same superposition of generations as in Fig.1b. One sees that the DE evolution thus far has produced a *range* of configurations, all having cost  $\chi$  comparable to the single value found by the Stellopt-LM runs, and with best value  $\chi_b \approx 6.41$ , slightly better than the best  $\chi_{LM} \approx 6.43$  produced by the LM searches.

From the numerous searches with Stellopt-LM carried out by the NCSX team, a number of different fixed-boundary QA configurations with promising characteristics have been identified. One would like to know how these (and other) configurations are related to each other, how different they are from each other, and whether there might be other QA configurations in  $\mathbf{z}$  space, as yet undiscovered, which are comparably or perhaps more attractive than those already found. In addition to the current NCSX reference configuration LI383,[8] here we shall also make use of 4 additional QAS configurations, all having  $N_{fp}=3$  field periods and fairly low aspect ratio: PG2, a QAS developed by P. Garabedian to achieve good stability through a deep magnetic well, C82, an earlier reference configuration constrained to fit inside the PBX vacuum vessel, II75, a configuration obtained starting from LI383 with a greater target value of edge transform [ $\iota_a(\text{II75}) \approx .75$  at  $\beta=4\%$ , versus  $\iota_a(\text{LI383}) \approx .65$ ], and A4k2, a configuration obtained starting from C82 but with enhanced elongation, which improves kink stability.

For brevity, we refer to the resultant stellarators as configurations 1a-5a, in the order just given. These were developed targeting different objectives, and thus are local optima for differing sets of weights  $\{w_i\}$ . To compare them, we choose a single set  $\{w_i\}$ , and reoptimize using Stellopt-LM, resulting in configurations 1c-5c, which resemble 1a-5a, and lie near them in  $\mathbf{z}$  space. This convergence of Stellopt-LM to 5 distinct minima when started from 5 different locations in  $\mathbf{z}$  illustrates the tendency of local methods mentioned in the Introduction to become trapped in local, suboptimal minima.

As a second DE application, we now take the  $D=5$  subspace spanned by these 5 'seed' configurations  $\mathbf{z}^{1c-5c}$ , and allow Stellopt-DE to search this space. The selection of the space makes use of knowledge found using the LM optimizer, but the search within this space is unbiased, *i.e.*, the DE optimizer has no information on where these optima lie. From a best cost value  $\chi_b(g=0)=42.1$  at generation  $g=0$ ,  $\chi_b$  falls to 3.53 by  $g=16$ , and thereafter remains quite flat, reaching 3.47 by  $g=52$ , about 94% and 59%, respectively of  $\chi(\text{LI383}_c)=3.66$  and  $\chi(\text{A4k2}_c)=5.84$ , the lowest 2 of the 5 seed values. The configuration with the lowest  $\chi$  for  $g=52$  just mentioned lies only 1.0 cm from LI383\_c and 1.9 cm from the related II75\_c (the 2 lowest- $\chi$  c-configurations), versus 17.1 cm from A4k2\_c, where we introduce the simple norm  $|\mathbf{z}| \equiv (\sum_j z_j^2)^{1/2}$ . Thus, without information on the locus of the LM optima, the DE method modestly improves on the 5 local minima found previously by LM plus human interaction.

## Taxonomy and Mapping Studies

Configurations 1c and 4c lie quite near each other (unsurprising because configuration 4a derives from 1a), and these and 2c have a bullet-like shape with positive triangularity at  $\zeta=\pi$ , while the remaining 2 seeds, 3c and 5c also lie near each other (again unsurprising because 5a derives from 3a), and have negative triangularity and are indented around  $\theta=0$ . (See Fig.2.) Thus, the  $\zeta=\pi$  cross section

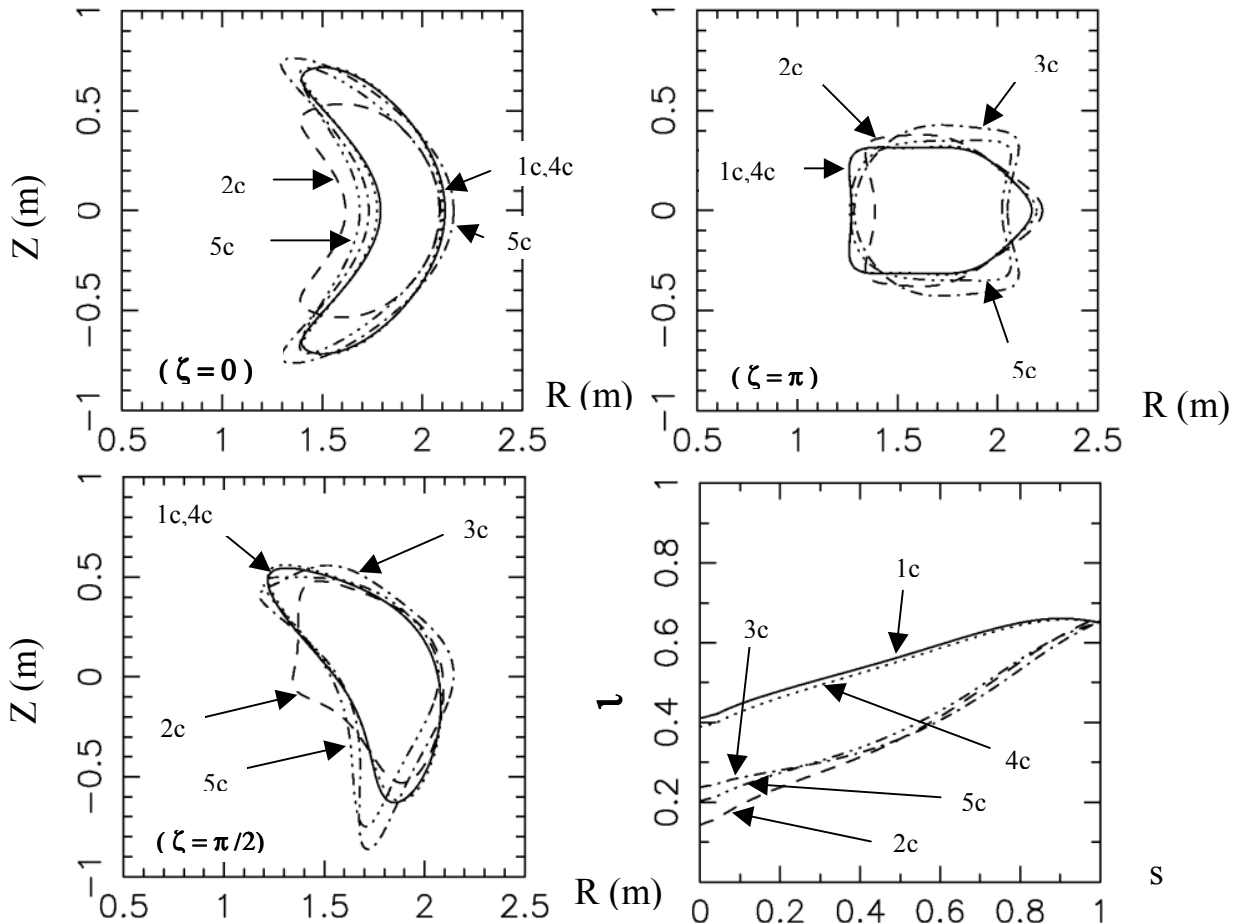


Figure 2

shapes suggest a division into 2 classes of configurations. A refinement of this simple picture is suggested by the  $t$  profiles for these 5 stellarators: as opposed to the larger value  $t_a(s=0) \approx .4$  of 1c and 4c, 2c instead has the smaller value 0.2 of 3c and 5c. An overall taxonomy suggested by these two characteristics is thus 1c and 4c in class A, 2c in hybrid class B, and 3c and 5c in class C.

Selecting one member of each of the related pairs results in 3 seed vectors representing each of these classes. Selecting 1c and 3c, we thus plot  $\chi$  over the 2-D space spanned by

$$\mathbf{z} = \mathbf{z}^{1c} + a_1(\mathbf{z}^{2c} - \mathbf{z}^{1c}) + a_2(\mathbf{z}^{3c} - \mathbf{z}^{1c})$$

for all values of coefficients  $a_{1,2}$ .

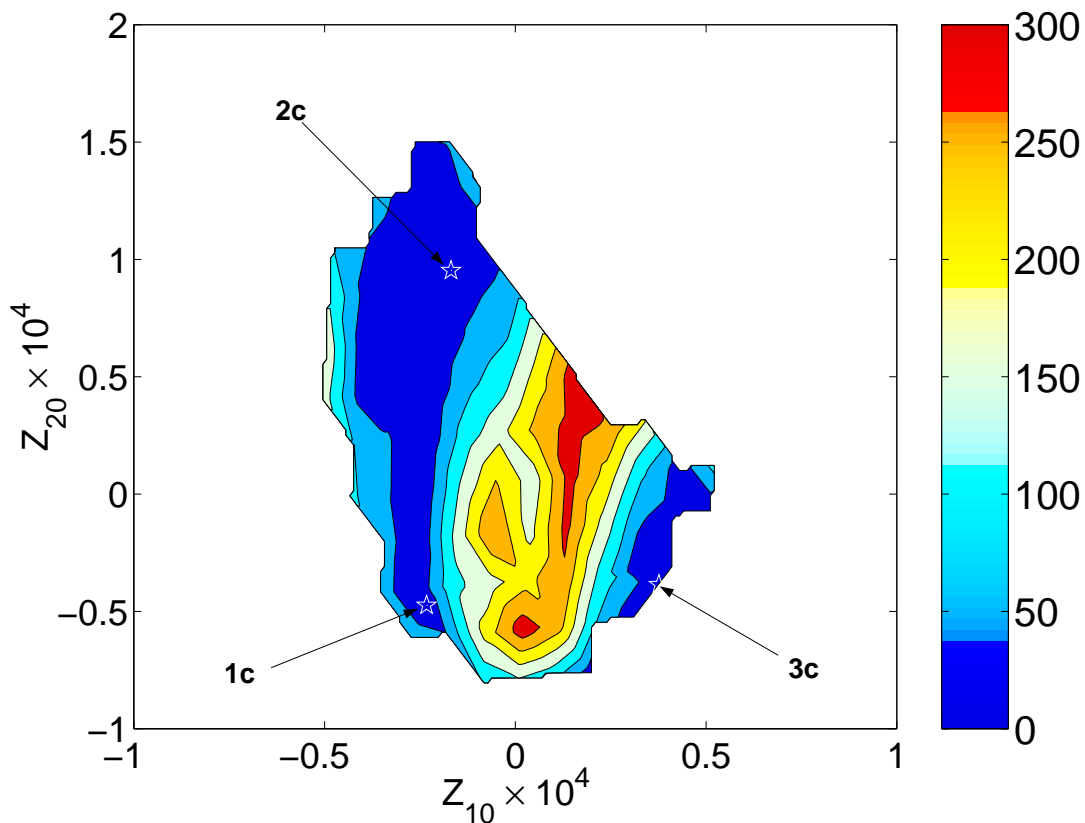


Figure 3

Accordingly, in Fig.3 is shown a contour plot of  $\chi$  over the  $(z_{10}, z_{20})$  plane. The choice of  $z_{10}$  and  $z_{20}$  is again arbitrary, and does not affect our conclusions. Choosing  $\mathbf{z}^{5c}$  instead of  $\mathbf{z}^{3c}$  as a basis vector also leaves the picture qualitatively the same. One observes a central 'ridge' running roughly vertically, with peak values around  $\chi \approx 300$ . Configurations 1c and 2c lie in a triangle-shaped valley to the left of this ridge ( $\chi$  in the range 0-50), and 3c lies in a second valley to its right. No values are given outside the curve bounding all the contours shown, because VMEC or sometimes TERPSICHORE fails to converge there. The configurations in this region are too exotic (and thus probably less realizable) for these codes to operate successfully. Thus, while Stellopt-LM has been searching an in-principle unbounded  $\mathbf{z}$  space, that space is bounded, and far smaller than one might have supposed, if one regards failure of VMEC or TERPSICHORE as a good indicator that the configuration is impractical. Moreover, across the limited range of practical configurations, one notes that  $\chi$  manifests only a few maxima and minima. This 2-D picture provides an explanation for the small number of attractive QAS classes which previous search has uncovered, included in the taxonomy just discussed.

Some insight into the physical origin of the topography of  $\chi$  may be seen from the breakdown into its component parts. One finds that  $\chi_K$  is by far the dominant factor, and thus that the central ridge is due to increased kink instability as configurations pass from the positive to negative triangularity form, with  $\chi_{Bmn}$  having a significant role only in the flat triangular valley of near kink stability.

## Discussion

As expected, we have found that Stellopt-DE is much less inclined to become trapped in local suboptimal minima than Stellopt-LM. A single run takes appreciably longer (typically a factor of 7-10) than a single LM-run. However, the LM optimizer typically must be run several times, with human adjustment between runs, in order to arrive at a good optimum. For the applications studied thus far, Stellopt-DE has found configurations improving modestly on those developed by the Stellopt-LM searches. We regard this as providing additional confidence that the LM+human approach the NCSX team has used to date to find good QAS configurations is working.

By examining a subspace which contains a range of quite different candidate configurations found earlier, we find a taxonomy of a small number of QAS classes into which the optimization runs fall, and a map on which this taxonomy and all the configurations examined can be placed, and the relationship among them viewed. We find 3 principal QAS classes, designated A, B and C, lying on the 2 sides of a ridge in  $\chi$ , which is produced by enhanced kink instability as the configurations deform from the positive triangularity at  $\zeta=\pi$  of classes A and B to the outward-indented, negative triangularity of class C. Class A is typified by LI383, the current NCSX reference design, class B by PG2, a design developed by Garabedian, and class C by A4k2 or C82, an earlier reference design.

This map indicates that the extent in components  $z_j$  over which one finds realizable configurations is not very large, when measured by the typical scale length  $L_j$  for  $\chi$  to go from a maximum to a minimum. This implies that the number of different QAS classes, as defined by the number of principal basins of  $\chi$  over the realizable region of  $\mathbf{z}$  space, is also not large, consistent with the small number (3) of main classes found in the present study. While further study is needed to solidify this picture, it is consistent with the accumulated record of searches thus far for attractive QA stellarators, and offers the possibility of a large reduction in the uncertainty and complexity of our understanding of stellarator configuration space.

**Acknowledgments:** The authors are grateful to S.P. Hirshman and E. Valeo for numerical advice and assistance, to A.H. Boozer and L.-P. Ku for useful discussions, and to M. Zarnstorff for bringing the DE method to our attention. This work supported by U.S. Department of Energy Contract No.DE-AC02-76-CHO3073.

## References

- [1]J. Nührenberg, R. Zille, *Phys. Lett.* **114A**, 129 (1986).
- [2]J.N. Talmadge, V. Sakaguchi, F.S.B. Anderson, D.T. Anderson and A.F. Almagri, *Phys. Plasmas* **8**, 5165 (2001).
- [3]A. Reiman, G. Fu, S. Hirshman, D. Monticello, H. Mynick, et al., *European Physical Society Meeting on Controlled Fusion and Plasma Physics Research*, Maastricht, the Netherlands, June 14-18, 1999, (European Physical Society, Petit-Lancy, 1999).

[4] Wm. H. Press, et al., *Numerical Recipes in Fortran 77*, (Cambridge University Press, 1996), p.676ff.

[5] R. Storn, K. Price, *Dr. Dobb's Journal* **22**, 18 (1997). See also website [www.icsi.berkeley.edu/~storn/code.html](http://www.icsi.berkeley.edu/~storn/code.html) for links to related work on the DE method.

[6] H.E. Mynick, N. Pomphrey, S. Ethier, (to appear in *Phys. Plasmas*).

[7] D.E. Goldberg, *Genetic Algorithms in Search, Optimization, and Machine Learning*, (Addison-Wesley, Reading, MA, 1989).

[8] National Compact Stellarator Team, National Compact Stellarator Experiment Physics Validation Report, <http://www.pppl.gov/ncsx/pvr/pvr.html>, (March, 2001).